Shale gas reservoir characterization workflows

Satinder Chopra*, Arcis Seismic Solutions, Calgary, Canada
schopra@arcis.com
Ritesh Kumar Sharma, Arcis Seismic Solutions, Calgary, Canada
and
Kurt J. Marfurt, The University of Oklahoma, Norman, OK, USA

Summary

As shale gas resources have emerged as a viable energy source, their characterization has gained significance. The organic content in these shales which are measured by their TOC ratings, influence the compressional and shear velocities as well as the density and anisotropy in these formations. Consequently, it should be possible to detect changes in TOC from the surface seismic response. Besides TOC, different shale formations have different properties in terms of maturation, gas-in-place, permeability, and brittleness. We discuss different workflows for characterizing shale formations that involve well log data as well as seismic data.

Introduction

In the last decade and more, shale gas resources have emerged as a viable energy source. This became possible after the Mississippian Barnett Shale in the Fort Worth Basin was successfully developed with the application of hydraulic fracturing and horizontal drilling. Logically, geoscientists began to look for other shale basins in the US and soon the Devonian Antrim shale of the Michigan Basin, the Devonian Ohio Shale of the Appalachian Basin, the Devonian New Albany Shale in the Illinois Basin and the Cretaceous Lewis Shale in San Juan Basin were explored and developed. Following these, the Fayetteville Shale in Arkansas and the Woodford Shale in Oklahoma were developed in 2004, followed by Haynesville Shale developed in 2008.

The development of these shales changed the traditional approach geologists had been following – that of the sequence of gas first being generated in the source rock, followed by its migration into the reservoir rock in which it is trapped. Shale-gas formations are both the source rocks and the reservoir rocks. There is no need for migration and since the permeability is near zero, it forms its own seal The gas may be trapped as free gas in natural fractures and intergranular porosity, as gas sorbed into kerogen and clay-particle surfaces, or as gas dissolved in kerogen and bitumen (Curtis, 2002). The shale gas reservoirs are characterized by low production rates (20-500 Mcf/d) but are usually spread over large areas and are up to 450 m thick. They are organically rich with total organic carbon content (TOC) varying from 1 to 20 wt%, such that the reservoirs contain large gas reserves (2 to 20 bcf/km^2). Shale gas reservoirs rely on natural fractures for porosity and permeability as the matrix porosity or permeability is low. In the absence of natural fractures, these reservoirs need stimulation by way of hydraulic fracturing. Compared to conventional reservoirs, shale gas reservoirs have low recovery factors (~20%). For the wells drilled into these reservoirs, the initial decline rates are rapid (~70%) but bottom out gradually (~6%) in later years (EIA document, 2011).

For a shale gas reservoir to become a successful shale gas play, the following characteristics need to be considered: (a) organic richness (TOC), (b) maturation (R_o%), (c) thickness, (d) gas-in-place, (e) permeability, (f) mineralogy, (g) brittleness, and (h) pore pressure. Besides all these the depth of the shale gas formation should also be considered as it will have a bearing on the economics of the gas recovery. An optimum combination of these factors leads to favorable productivity.

As different shale gas reservoirs have different properties, it is imperative to study them before any exploitation plan is put in place. In Figure 1 we show a comparison of some of these factors for five different shale gas reservoirs. Notice the differences in each of them. Another important point to consider is that such properties can be determined at the location of the wells where the well log and core data are available. However to characterize the shale gas formations different geophysical workflows need to be used on 3D surface seismic data. We discuss some of these workflows below.

Using well log data

As resistivity increases significantly in mature rocks due to the generation of nonconducting hydrocarbons, it can be detected easily on the resistivity log curves. Passey et al. (1990) proposed the $\Delta \log R$ technique for measuring TOC in shale gas formations which are valid over a wide range of maturities. In this technique the transit time curve and the resistivity curves are scaled in such a way that their relative scaling is -100 µs/ft per two logarithmic resistivity cycles. In this case, the two curves overlie each other over a large depth range, except for organic-rich intervals where they would appear separated by $\Delta \log R$, which in turn is linearly related to TOC, and is a function of maturity. The level of maturity (LOM) is usually obtained from sample analysis where the vitrinite reflectance (R_o%) method is commonly used for the purpose. LOM values derived from R% are seen to vary from 6 or 7 to 12 depending on the type of organic matter, with 7 indicating the onset of maturity for oil-prone kerogen and 12 indicating the onset of overmaturity for oil-prone kerogen. To the left of Figure 2 we show the sonic and resistivity curves indicating the $\Delta \log R$ separation.

Attributes generated from the available log curves (sonic, density, resistivity and porosity) need to be crossplotted to gain more insight into the shale reservoir and determine which attributes would be suitable to distinguish the reservoir from the non-reservoir zones.

Løseth et al. (2011) have shown that a relationship between TOC values and acoustic impedance can be obtained by crossplotting measurements made from cores and well logs. Such a relationship can then be used to transform acoustic impedance volumes derived from simultaneous inversion into TOC volumes.

Using seismic data

TOC changes in shale formations influence V_P, V_S, density and anisotropy and thus should be detected on the seismic response.

1. Carcione (2001) showed that for a given layer thickness and kerogen content, the PP reflection coefficient decreases with increasing angle. This implies that if the near and far stack are examined for a given seismic data volume, at the top of the reservoir rock the negative amplitudes on the near stack will be seen as dimmed on the far stack, exhibiting a class-IV AVO response. Similarly, the base of the reservoir zone will exhibit a distinct positive reflection that will also dim with offset, giving rise to a class-I AVO response. This is expected since the

acoustic impedance for shale reservoir rocks with TOC > 4% is lower than the same rocks without TOC. Such a simple exercise allows separation of reservoir facies from the non-reservoir ones.

Impedance curves from wells that penetrate the shale strata, when put together on the same plot exhibit reservoir quality variations (Treadgold et al., 2011; Løseth et al., 2011). Zones associated with higher organic content are associated with lower acoustic impedance values and could be picked up from such a display. Such an exercise should form a preliminary workflow.

2. Rickman et al. (2008) showed that brittleness of a rock formation can be estimated from well log curves of Poisson's ratio and Young's modulus. This suggests a workflow for estimating brittleness from 3D seismic data, by way of simultaneous prestack inversion that yields Z_P, Z_S, V_P/V_S, Poisson's ratio, and in some cases meaningful estimates of density. Zones with high Young's modulus and low Poisson's ratio are those that would be brittle as well as have better reservoir quality (higher TOC, higher porosity). Such a workflow works well for good quality data.

3. One hybrid workflow entails the generation of curvature volumes as well as relative acoustic impedance from thin-bed reflectivity (Chopra et al., 2006). Thin-bed reflectivity is a reflection coefficient volume derived from the input seismic data by means of spectral inversion. As there is no seismic wavelet in this volume, the relative acoustic impedance obtained from this volume has a higher level of detail. In Figure 3 we show a chair display of a horizon slice through a k_1 most-positive principal curvature volume with a vertical slice through the corresponding seismic amplitude volume, which indicates lineaments correlated to fractures at that level. In Figure 4 we show an overlay of the hypothesized fracture network over the relative impedance display. Notice the different curvature lineaments appear to fall into the appropriate high impedance pockets separating them from low impedance pockets, may be suggesting cemented fractures.

4. Natural fractures in shale formations can provide permeability pathways and so need to be characterized, if they exist. While many shale formations may be devoid of such natural fractures, others such as the Woodford Shale is hard and faulted. The Eagle Ford Shale as well as the Muskwa-Otter-Park–Evie Shale package in the Horn River Basin also exhibit natural fractures. Such fractures could be characterized by running the discontinuity attributes (coherence and curvature) on post-stack data or by utilizing prestack processes such as AVO/AVAz/VVAz. Natural fractures in the shale formations can be detected by examining azimuthal variations of the velocity/impedance field, e.g. normalized V_{fast}-V_{slow} (Treadgold et al., 2011; Zhang et al., 2010).

5. Seismic waveform classification is another quick and easy method that holds promise as an application for shale gas reservoir characterization. It essentially classifies seismic waveforms in the interval of interest based on their shapes. Usually the traces are grouped into classes and displayed in color such that each class has its own color. The resulting map exhibits seismic facies variation and enables demarcation of favorable zones from the others. The waveform classification process could be unconstrained or constrained depending on how the waveforms are subdivided. In Figure 5 we show the result of unconstrained waveform classification and compare it with an equivalent display from the relative acoustic impedance derived from thin-bed reflectivity. The two displays compare favorably.

Figure 1: Description of chart, graphic, equation, etc.

Conclusions

Geophysical methods can help in characterizing the shale gas resource plays. However, the methodology adopted is in general quite different from methodologies applied to conventional reservoirs. In addition, the characterization of each shale reservoir could require particular types of tools and have to be applied with care. While we have discussed a number of different workflows for characterization of shale gas reservoirs, the choice of such methods would continue to evolve to meet the growing challenges and expectations.
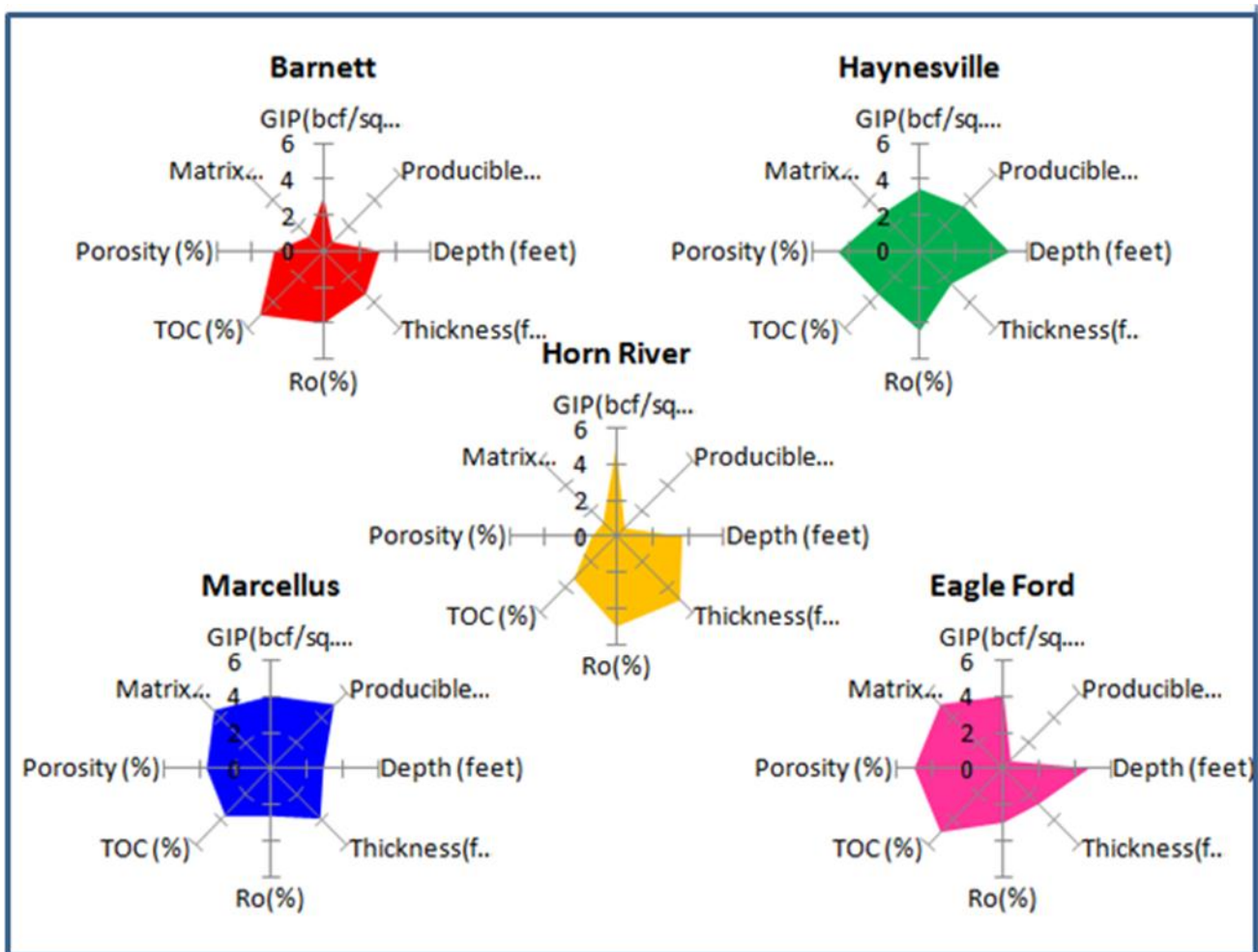
Figure 1: Comparison of shale characteristics for five different types of shale reservoirs. Notice the variation in the eight properties considered. (After Roth, 2010).
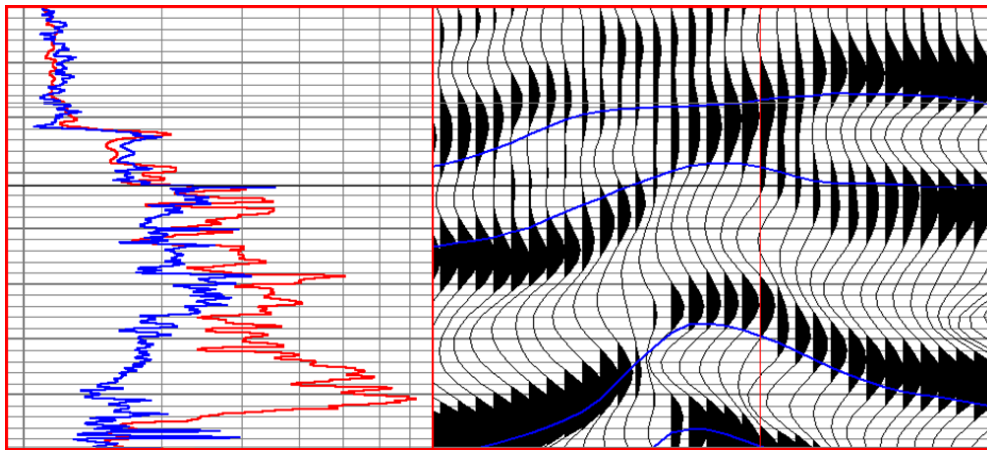
Figure 2: Log data in the form of transit time (blue) and resistivity (red) show a separation for ΔlogR which is indicative of high TOC. The location of the curves is the vertical green line on the seismic section.
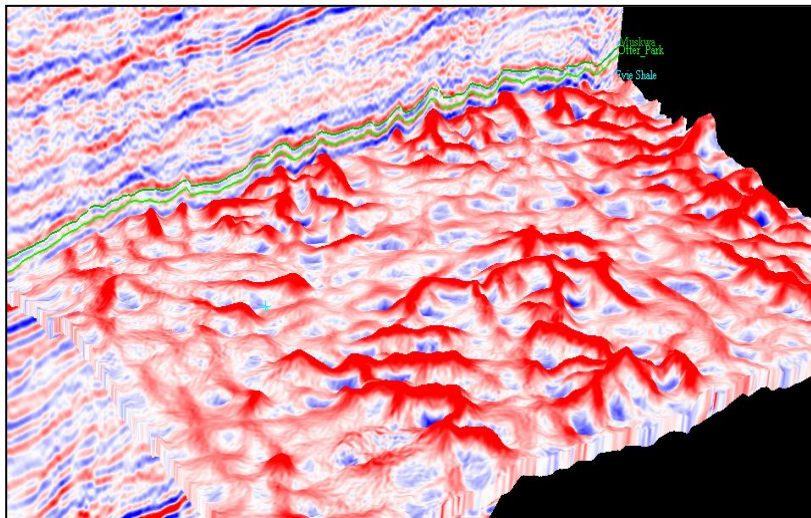

Figure 3: Chair display showing a vertical slice through seismic amplitude and a horizon slice through the k_1 most-positive principal curvature. Notice the correlation of the different lineaments on the curvature with their seismic signatures.
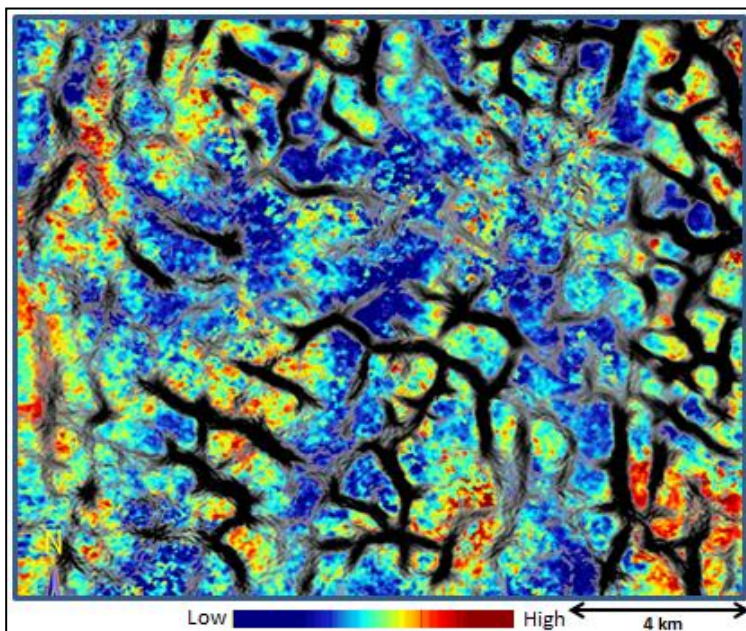

Figure 4: A horizon slice at the Muskwa level through the relative acoustic impedance volume derived from thin-bed reflectivity inversion of 3D seismic data co-rendered with most-positive curvature lineaments using transparency.
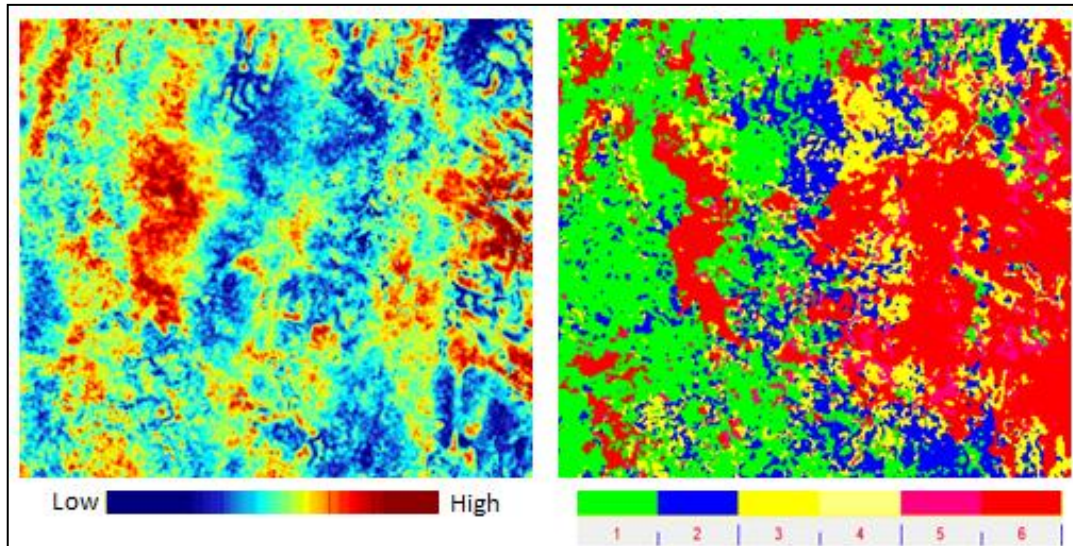
Figure 5: A horizon slice at the Evie Shale level from (left) the relative acoustic impedance volume derived from thin-bed reflectivity inversion of 3D seismic data, and (right) from waveform classification of a window extending 20 ms below the Evie-Shale marker. Notice the overall pattern of the red color seems to follow the pattern seen on the high impedance see on the left.

Acknowledgements

References

Carcione, J., 2001, AVO effects of a hydrocarbon source- rock layer: Geophysics, **66**, 419-427.

Chopra, S., J. P. Castagna and O. Portniaguine, 2006, Seismic resolution and thin-bed reflectivity inversion, CSEG RECORDER, **31**, 19-25.

Curtis, J. B., 2002, Fractured shale gas systems: AAPG Bulletin, **86**, 1921-1938.

EIA document, 2011, Review of emerging resources: US shale gas and shale oil plays, available at ftp://ftp.eia.doe.gov/natgas/usshaleplays.pdf, accessed on 4th April, 2012.

Løseth, H., L. Wensaas, M. Gading, K. Duffaut, and M. Springer, 2011, Can hydrocarbon source rocks be identified on seismic data?: Geology, **39**, 1167-1170.

Passey, Q. R., S. Creaney, J. B. Kulla, F. J. Moretti, and J. D. Stroud, 1990, A practical model for organic richness from porosity and resistivity logs: AAPG Bulletin, **74**, 1777-1794.

Rickman, R., M. Mullen, E. Petre, B. Grieser, and D. Kundert, 2008, A practical use of shale petrophysics for stimulation design optimization: All shale plays are not clones of the Barnett Shale, SPE paper 11528.

Treadgold, G., B. Campbell, B. McLain, S. Sinclair and D. Nicklin, 2011, Eagle Ford shale prospecting with 3D seismic data within a tectonic and depositional system framework, The Leading Edge, **30**, 48-53.

Zhang, K., B. Zhang, J. T. Kwiatkowski, and K. J. Marfurt, 2010, Seismic azimuthal impedance anisotropy in the Barnett Shale: 80th Annual International Meeting of the SEG, Expanded Abstracts **29**, 273-277.